Classifying Vehicle Cornering Behavior using Mobile Sensor Data

Aristotelis Tsoutsanis, George Yannis

Department of Transportation Planning and Engineering – National Technical University of Athens, Athens, Greece

18 January 2025

Abstract

This paper presents a methodology to classify cornering behavior in vehicles using data from mobile devices equipped with accelerometers and gyroscopes. Data was captured from a fixed-position device on a vehicle, collecting accelerometer (3 axes), gyroscope (3 axes), and GPS speed. Two driving modes were analyzed: Normal and Aggressive, with data collected from over 100 trips. The paper describes aligning the device's coordinate system with the vehicle's, preprocessing data through peak detection, augmentation, and downsampling, and applying a four-layer Long Short-Term Memory (LSTM) network to classify cornering as normal or harsh. Experimental results demonstrate the model's effectiveness, achieving 84% accuracy in distinguishing driving cornering behaviors.

1 Introduction

Road safety data sources are essential for understanding the causes of crashes and predicting future risks to reduce road traffic accidents. Various factors, including driving speed, road infrastructure, and driver behavior, influence crashes. However, crashes are relatively rare, making it challenging to detect and assess road safety conditions in real-time. To address this challenge, researchers have employed crash surrogates in road safety studies in order to define crash proneness and associate it with crash risk [1, 2].

Recent advancements in sensor technology and smartphone-based systems now enable large-scale monitoring of driving behaviors. Smartphones, equipped with sensors such as accelerometers, gyroscopes, and GPS, generate rich datasets for analyzing vehicle dynamics. High G-force events, characterized by vehicle acceleration exceeding expected levels, typically result from hard braking or abrupt acceleration maneuvers. These events are widely used by researchers to evaluate driver behavior and identify high-risk drivers [3].

Previous studies, such as [4], have explored smartphone-based detection of hard-braking events to enhance road safety services, demonstrating the potential of mobile sensors in real-world driving scenarios. Additionally, the use of gyroscopes in mobile applications, as discussed in [5], has shown promise in capturing rotational motion, making it a valuable tool for detecting cornering events.

The accurate classification of vehicle cornering behaviors (e.g., normal vs. harsh turns) is crucial for a wide range of applications, including driver behavior analysis, autonomous driving systems, and vehicle safety enhancement. Identifying and mitigating harsh driving maneuvers is particularly significant, as these actions can lead to severe vehicle instability. For example, while rollover incidents constitute only 3% of all vehicle crashes, they account for nearly one-third of passenger fatalities, highlighting the critical risks associated with extreme driving events [6]. The ability to detect and analyze these behaviors in real-time could play a pivotal role in reducing fatalities and improving road safety.

In this work, we leverage mobile sensor data—including accelerometer, gyroscope, and GPS speed—to develop a machine learning model capable of classifying cornering events as either normal or aggressive. The data was collected using a mobile device mounted in a fixed position on the vehicle, capturing real-time sensor readings at varying sampling rates: 5 Hz for accelerometer and gyroscope data, and 1 Hz for GPS data. This study encompasses the entire pipeline of data processing, including preprocessing raw data, aligning coordinate systems, detecting cornering events through peak analysis, and training a robust classifier.

2 Methodology

2.1 Data Collection

The data used in this study consists of accelerometer (3 axes), gyroscope (3 axes), and GPS speed captured from a mobile device mounted in a fixed position inside a vehicle as shown in Figure 1a. Data were collected from over 100 trips and $\sim 588,904$ mobile readings in two different driving modes: Normal and Aggressive, from three drivers, each with over 6 years of driving experience. The driving sessions took place in Athens, Greece, covering a mix of urban and suburban road conditions, with areas characterized by residential, commercial and light industrial land use. The sampling rates of accelerometer and gyroscope data were set to 5 Hz, while GPS speed was recorded at 1 Hz.

2.2 Coordinate System Alignment

The first step in preprocessing the data was to align the phone's coordinate system as shown in Figure 1b, denoted as coordinate system 2, to the vehicle's coordinate system, denoted as coordinate system 1, specifically along the Y-axis. To facilitate this, we captured a 4-second data segment with the mobile device mounted on the vehicle while it was stationary on a flat surface. This stationary calibration period allowed us to calculate the angles of misalignment between the two coordinate systems and thus construct the rotation matrix R_{21} for the transformation of collected data from the phone's coordinate system to that of the vehicle's; as shown in eq. 1.

$$\begin{bmatrix} x \\ y \\ z \end{bmatrix}_1 = R_{21} \begin{bmatrix} x \\ y \\ z \end{bmatrix}_2 \tag{1}$$

Note that the rotation matrix R_{21} can be analytically described through the angles of rotation, these being angles θ, κ and ψ around the 3 axes x, y, z; as shown in eq. 2.

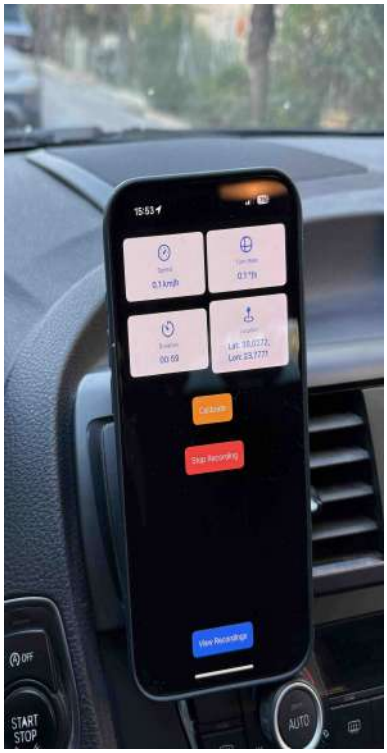

(a) Mobile device mounted in the car.

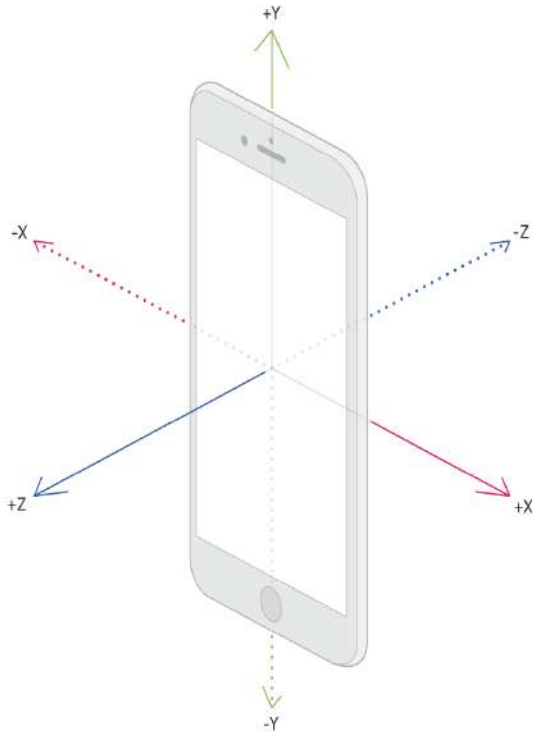

(b) Device coordinate system.

Figure 1: (a) Mobile device mounted in the car and recording a trip; (b) Illustration of a mobile device coordinate system. Source: developer.apple.com/documentation.

$$
\begin{aligned}
R_{21} &= R_{x_{21}}(\theta) \cdot R_{y_{21}}(\kappa) \cdot R_{z_{21}}(\psi) = \\
&= \begin{bmatrix} 1 & 0 & 0 \\ 0 & \cos\theta & -\sin\theta \\ 0 & \sin\theta & \cos\theta \end{bmatrix} \cdot \begin{bmatrix} \cos\kappa & 0 & \sin\kappa \\ 0 & 1 & 0 \\ -\sin\kappa & 0 & \cos\kappa \end{bmatrix} \cdot \begin{bmatrix} \cos\psi & -\sin\psi & 0 \\ \sin\psi & \cos\psi & 0 \\ 0 & 0 & 1 \end{bmatrix}
\end{aligned} \tag{2}
$$

Considering the above definitions, the unknown rotation matrix R_{21} can be estimated through an optimization scheme as shown in Algorithm 1.

Algorithm 1 Optimization Algorithm for computing rotation matrix

1: **Compute Rotation Matrix to Align Gravity:**
Require: Captured vector $\mathbf{g} = [g_x, g_y, g_z]^T$ ▷ Coordinate system 2
2: initial_guess $\leftarrow [0, 0, 0]$ ▷ Initial rotational angles
3: target vector $\mathbf{t} \leftarrow [0, -1, 0]^T$ ▷ Coordinate system 1
4: R $\leftarrow \min(||\mathbf{t} - R_{21} \cdot \mathbf{g}||^2, \text{initial\_guess})$
5: **return** R

To ensure the accuracy and reliability of the proposed method for constructing the rotation matrix R_{21}, we conducted a rigorous testing phase. The primary goal was to validate the method against cases where the true rotation matrix was already known. This allowed us to verify whether the method produced an optimal and correct solution under controlled conditions.

2.3 Peak Detection and Time-Series Creation

To identify cornering events, we focused on detecting peaks in the gyroscope's Y-axis, as turns are expected to generate significant spikes in this data as shown in Figure 2. Before peak detection, a data smoothing step was applied to the gyroscopic measurements along the Y-axis to reduce noise and improve the reliability of peak identification. The smoothing was performed using a simple moving average technique. Based on experimental findings, we defined cornering events by identifying all peaks with greater than or equal to 0.2 radians per second. For each peak, a multi-variate time-series window of ± 1 seconds was extracted, which corresponds to a complete cornering event. These windows were labeled as either normal or aggressive based on the driving mode.

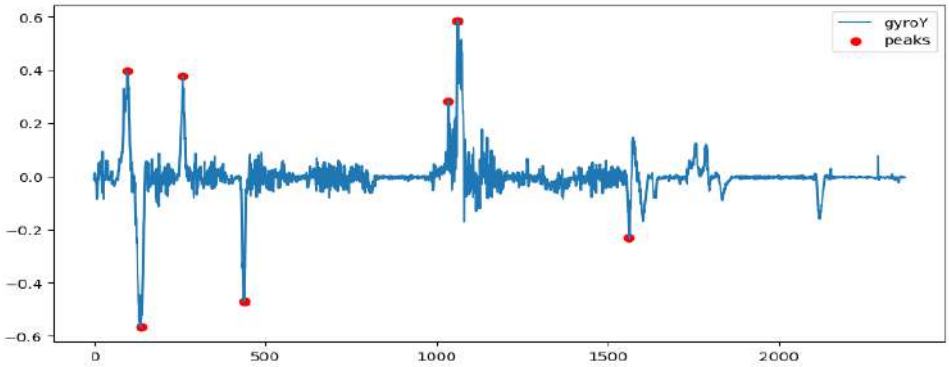

Figure 2: Gyroscope Y-axis with peak detection.

Figure 3 illustrates the map of identified turns and corners in the dataset, providing a spatial overview of the locations where cornering/turns events were detected.

2.4 Cornering Augmentation

To address the imbalance in the dataset, where aggressive cornering events were underrepresented compared to normal ones, we implemented a data augmentation technique. Aggressive cornering events were augmented by flipping their gyroscope-Y readings, simulating turns in the opposite direction and generating new instances of aggressive events.

2.5 Final Dataset Composition

After the cornering augmentation, normal turns were downsampled to balance the dataset, ensuring that both classes had an equal representation in training. The final dataset consists of a balanced set of 1212 normal and 1212 aggressive turns, with each turn represented as a 2-second multivariate time series. Each series captures the relevant sensor data needed to analyze the cornering behavior.

Figure 4 provides a detailed visualization of the data distributions for key features across the two classes:

1. Gyroscope Y-axis (gyroY): Captures rotational movements during cornering.
2. Speed: Indicates the velocity of the vehicle during turns.

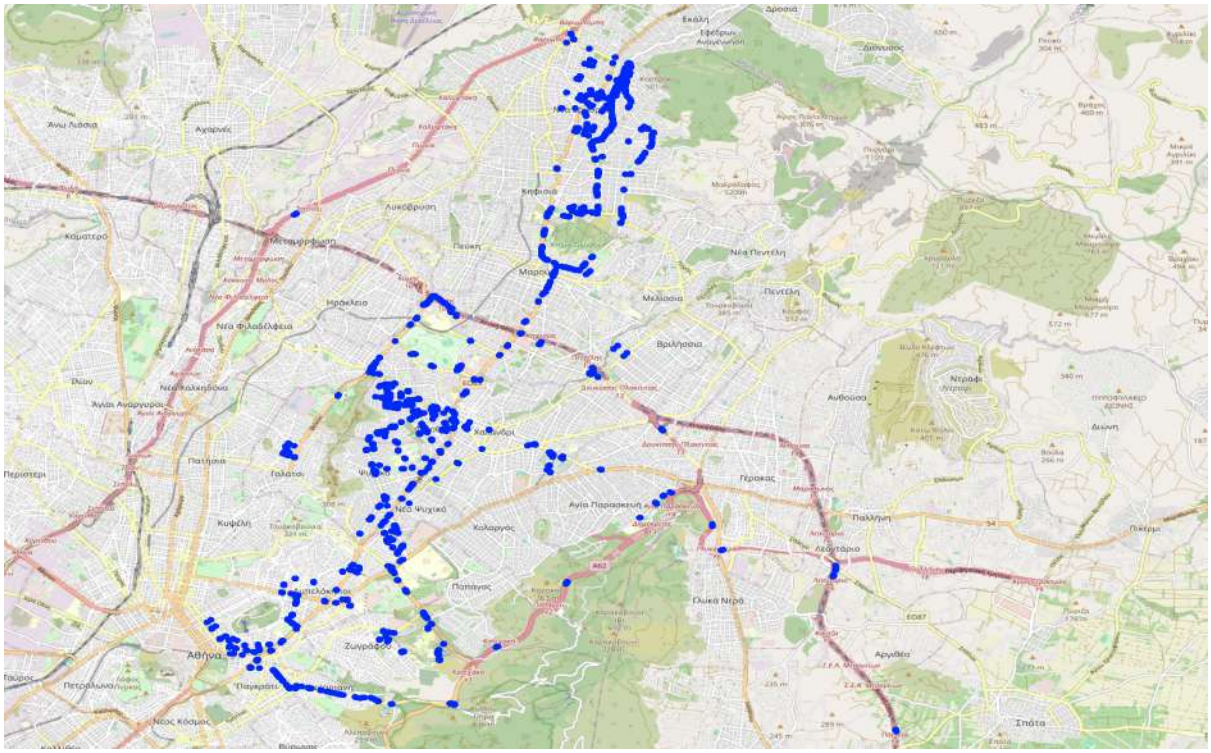

Figure 3: Map displaying detected turns/corners in the dataset.

3. Accelerometer Magnitude: Reflects the overall acceleration forces experienced during cornering.

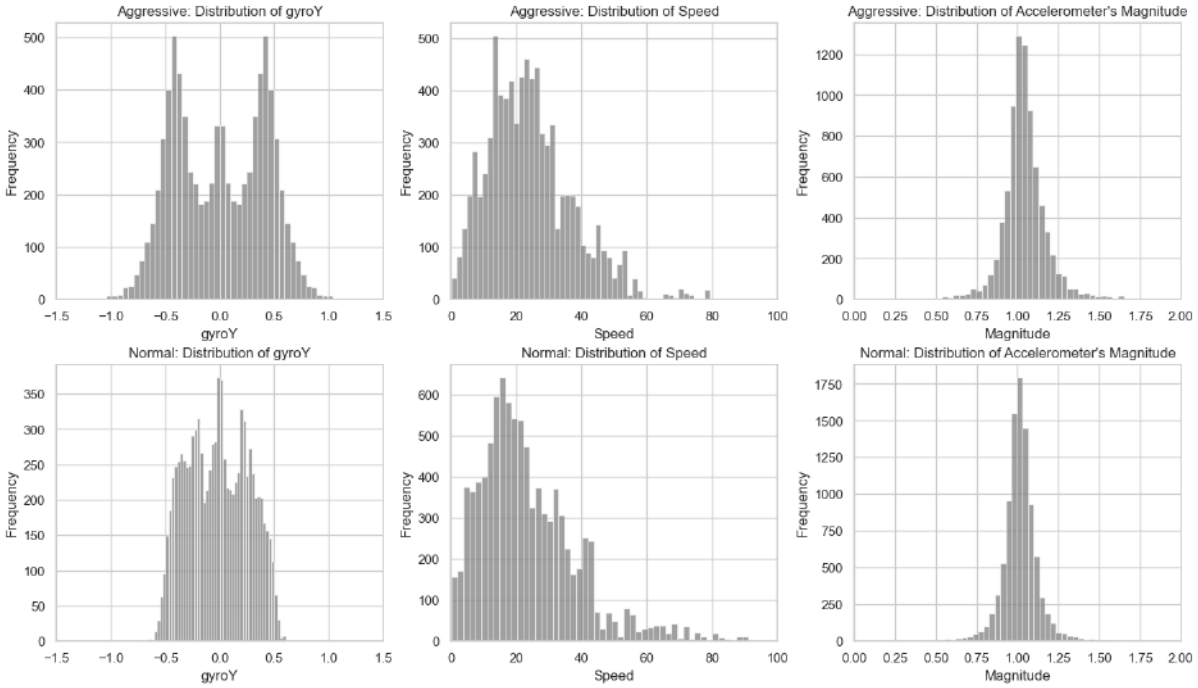

Figure 4: Distribution of normal and aggressive turns in the final dataset.

2.6 Model Architecture

The model used to classify cornering events is a Long Short-Term Memory (LSTM) network [7]. Specifically, a four-layer LSTM model, meaning stacking four LSTMs together to form a stacked LSTM, was chosen due to its ability to capture temporal dependencies in sequential data, which is essential for accurately classifying time-series data. The input features to the LSTM include the timestamps and the corresponding sensor readings (accelerometer's magnitude, gyroscope-Y, GPS Speed). The output of the stacked LSTM is passed through a fully connected linear layer, which maps the temporal features to the final class labels.

3 Experiments and Results

3.1 Training Setup

The LSTM model was trained using the augmented and downsampled dataset. The training was carried out with a training-validation split of 80-20%. The model was evaluated using a combination of performance metrics, including accuracy, precision, recall, and F1 score, each offering different perspectives on classification performance.

The following metrics were used to evaluate the model:

- **Accuracy**: Measures the proportion of correctly classified instances out of the total number of samples. It is calculated as:

$$\text{Accuracy} = \frac{TP + TN}{TP + TN + FP + FN}$$

  where TP, TN, FP, and FN denote true positives, true negatives, false positives, and false negatives, respectively.

- **Precision**: Focuses on the quality of positive predictions by measuring the proportion of true positives among all predicted positives:

$$\text{Precision} = \frac{TP}{TP + FP}$$

  Higher precision indicates fewer false positives, which is crucial for minimizing misclassification of normal cornering as aggressive.

- **Recall**: Also known as sensitivity or true positive rate, recall quantifies the proportion of actual positives correctly identified:

$$\text{Recall} = \frac{TP}{TP + FN}$$

  High recall ensures that most aggressive cornering events are correctly detected.

- **F1 Score**: The harmonic mean of precision and recall, balancing both metrics:

$$F1 = 2 \times \frac{\text{Precision} \times \text{Recall}}{\text{Precision} + \text{Recall}}$$

  This metric provides a single score that balances precision and recall, useful when there is an uneven class distribution or when both false positives and false negatives are costly.

3.2 Results

The model achieved a classification accuracy of 84.01% on the test set. The precision (84.61%) and recall (85.27%) indicate satisfactory performance in identifying both normal and aggressive cornering events.

Since both false positives and false negatives are undesirable, it is important to balance precision and recall. In this task, high recall ensures that aggressive cornering events are detected reliably, while high precision minimizes false alarms. The F1 score of 84.94% captures this balance, providing a more comprehensive measure of model performance than accuracy alone.

4 Conclusion

In this paper, we proposed a method for classifying cornering behavior using sensor data from mobile devices mounted on vehicles. Through data preprocessing, including coordinate system alignment, peak detection, and augmentation, we prepared a dataset suitable for training an LSTM model. The experimental results demonstrate that the LSTM model is capable of accurately classifying cornering events as either normal or aggressive, achieving promising results in terms of classification accuracy and F1 score.

The analysis of sharp cornering behavior has clear implications for road safety. Aggressive cornering is often linked to increased risks of accidents, excessive vehicle wear, and reduced fuel efficiency. By identifying and classifying these events, this research offers a practical step toward understanding driving patterns that contribute to unsafe conditions. The findings can also inform discussions about improving road safety measures and optimizing existing traffic management systems to reduce the likelihood of hazardous driving while also providing valuable insights for policymakers and insurance companies.

Future work will involve fine-tuning the model, and expanding the dataset to encompass a broader range of driving scenarios and conditions. Additionally, adding features related to road infrastructure, such as speed limits, road curvature, and surface conditions, could enhance the model's robustness and applicability.

Acknowledgements

This research has been conducted within the IVORY project. The project has received funding from the European Union's Horizon Europe research and innovation programme under grant agreement No 101119590.

References

[1] D. M. Gettman, Lili Pu, Tarek Sayed, and Steven G. Shelby. Surrogate safety assessment model and validation: Final report. 2008.

[2] Dimitrios Nikolaou, Apostolos Ziakopoulos, and George Yannis. A review of surrogate safety measures uses in historical crash investigations. *Sustainability*, 15(9), 2023.

[3] Bruce Simons-Morton, Kyeongmi Cheon, Feng Guo, and Paul Albert. Trajectories of kinematic risky driving among novice teenagers. *Accident; analysis and prevention*, 51C:27–32, 11 2012.

[4] Luyang Liu, David Racz, Kara Vaillancourt, Julie Michelman, Matt Barnes, Stefan Mellem, Paul Eastham, Bradley Green, Charles Armstrong, Rishi Bal, Shawn O'Banion, and Feng Guo. Smartphone-based hard-braking event detection at scale for road safety services, 2022.

[5] Christopher Barthold, Kalyan Pathapati Subbu, and Ram Dantu. Evaluation of gyroscope-embedded mobile phones. In *2011 IEEE International Conference on Systems, Man, and Cybernetics*, pages 1632–1638, 2011.

[6] Jeya Padmanaban and Stein Husher. Occupant injury experience in rollover crashes: an in-depth review of NASS/CDS data. *Annu Proc Assoc Adv Automot Med*, 49:103–118, 2005.

[7] Sepp Hochreiter and Jürgen Schmidhuber. Long short-term memory. *Neural computation*, 9:1735–80, 12 1997.